Resource allocation in downlink SWIPT-based cooperative NOMA systems

Longqi Wang and Ding Xu*
Wireless Communication Key Lab of Jiangsu Province
Nanjing University of Posts and Telecommunications, Nanjing 210003, China
[e-mail: xuding@ieee.org]
*Corresponding author: Ding Xu

Received May 22, 2019; revised June 27, 2019; accepted July 9, 2019; published January 31, 2020

Abstract

This paper considers a downlink multi-carrier cooperative non-orthogonal multiple access (NOMA) transmission, where no direct link exists between the far user and the base station (BS), and the communication between them only relies on the assist of the near user. Firstly, the BS sends a superimposed signal of the far and the near user to the near user, and then the near user adopts simultaneous wireless information and power transfer (SWIPT) to split the received superimposed signal into two portions for energy harvesting and information decoding respectively. Afterwards, the near user forwards the signal of the far user by utilizing the harvested energy. A minimum data is required to ensure the quality of service (QoS) of the far user. We jointly optimize power allocation, subcarrier allocation, time allocation, the power allocation (PA) coefficient and the power splitting (PS) ratio to maximize the number of data bits received at the near user under the energy causality constraint, the minimum data constraint and the transmission power constraint. The block-coordinate descent method and the Lagrange duality method are used to obtain a suboptimal solution of this optimization problem. In the final simulation results, the superiority of the proposed NOMA scheme is confirmed compared with the benchmark NOMA schemes and the orthogonal multiple access (OMA) scheme.

Keywords: Cooperative non-orthogonal multiple access, power splitting, simultaneous wireless information and power transfer, quality of service

http://doi.org/10.3837/tiis.2020.01.002 **ISSN : 1976-7277**

1. Introduction

Recently, the spectrum resources become more precious with the increasing demand for wireless transmission. As a new multiple-access technique, Non-Orthogonal Multiple Access (NOMA) has received a lot of attention in the upcoming 5G wireless networks because of its high spectral efficiency [1]-[4]. Different from the conventional orthogonal multiple access (OMA) which serves only one user within the same time or frequency, NOMA performs multiplexing in the power domain and allows multiple users to transmit information in the same time and frequency. The implementation of NOMA depends on superposition coding (SC) technique used at the transmitters to send signals of multiple users and successive interference cancellation (SIC) technique applied at receivers to eliminate the co-channel interference [5]. Since NOMA uses a new dimension to realize multiple access, it has the potential to improve the spectrum efficiency [6] as well as the energy efficiency [7]. The existing researches on NOMA mainly include the following aspects: NOMA with multiple-input multiple-output (MIMO) [8]-[10], cognitive radio inspired NOMA (CR-NOMA) [11]-[13], cooperative NOMA [14]-[16], etc. For example, in [8], the application of MIMO techniques to NOMA systems was considered and the ergodic capacity of the system was maximized subject to the constraints of total transmission power and minimum rate. In [11], the performance of CR-NOMA influenced by user pairing was studied compared with the fixed power allocation (PA) NOMA. According to SIC principle, the strong user decodes the message of the weak user before obtaining its own message. Hence, the strong user can act as a relay to forward the message of the weak user. In this context, reference [14] proposed a cooperative NOMA system and analyzed the outage probability and diversity order of this system.

Radio-frequency (RF) energy harvesting is a technology which can harvest energy from RF signals to power communication devices in energy constrained wireless network, such as Internet of Things (IoT) networks [17][18], low-power cognitive radio networks [19]-[21], and device-to-device networks [22]-[24]. In particular, simultaneous wireless information and power transfer (SWIPT) is a RF energy harvesting technology that can harvest energy and decode information from the same signal [25][26]. In [27], the problem of energy efficiency proportional fairness for SWIPT was investigated based on the stochastic geometry. In [28], cooperative resource allocation for SWIPT secondary users and primary users in cognitive radio networks was studied. Reference [29] proposed two relaying protocols for SWIPT based on the power splitting (PS) and time switching (TS) receiver architectures. For TS, the transmission time is divided into two portions for harvesting energy and transmitting information. For PS, the signals received by relay are divided into two portions for harvesting energy and transmitting information. In [30], the TS and PS schemes were considered in MIMO systems and some fundamental tradeoffs were revealed for maximizing the efficiency of simultaneous information and energy transmission. In [31], the TS and PS schemes were employed for the TDMA-based and OFDMA-based information transmission respectively. The author in [31] maximized the weighted sum-rate by optimizing the resource allocation under the minimum harvested energy constraint and the transmission power constraint. In [32], the outage performance of a multiuser OFDM system with SWIPT was investigated. Reference [33] proposed a novel protocol for energy harvesting cooperative communication systems based on a PS scheme and validated the average achievable capacity of the proposed protocol outperforms the existing PS protocol.

For cooperative NOMA, there is inevitably energy consumption when the near user forwards a signal to the far user. However, it is unreasonable for the energy-constrained near user to provide the energy used for forwarding the far user's signal. Hence, SWIPT can be applied at the near user for decoding information and harvesting energy simultaneously in cooperative NOMA systems and the harvested energy can be used for forwarding signals. Many works have been investigated to jointly consider NOMA and SWIPT, such as [34]-[37]. In [34], TS scheme was used to transfer information and energy for a MISO system with cooperative NOMA transmission, and the rate of the best-of-the-effort node was maximized by jointly optimizing the beamforming vectors, time and forwarding power, under the constraint of the passive node's QoS. Reference [35] proposed a new PS protocol for energy harvesting relay and studied its impact on the outage performance of users in a cooperative NOMA system with SWIPT. In [36], the authors adopted a PS scheme to assist the weak user, and jointly optimized the beamforming vectors and the PS ratio to maximize the transmission rate at the strong user, limited by the QoS requirement of the weak user in the MISO and SISO NOMA cases, respectively. In [37], a new cooperative NOMA protocol based on SWIPT was proposed, and the outage probability and the diversity of all users were derived to verify the performance of the proposed protocol. As far as we know, most of the existing researches considered there exists direct link between the information source and the far user in SWIPT assisted cooperative NOMA systems. However, there are situations where the far users who are outside the coverage of the information source want to communicate. Therefore, it is necessary to consider the case where no direct link exists between the far user and the information source. It is worth pointing out that in [38], a downlink NOMA system with no direct link between the far user and the source was considered, and the near user was proposed to act as a full-duplex relay for the information transmission of the far user. In [38], the author minimized the outage probability of the system and maximized the minimum rate of the two users by jointly optimizing the transmission power of the near user and the PA parameters of different users' signals. However, RF energy harvesting was not considered in [38]. To the best of our knowledge, cooperative NOMA systems using SWIPT where the far user is out of the coverage of the BS have not been investigated yet. This motivates the research in this paper.

In this paper, a SWIPT assisted downlink cooperative NOMA transmission system consisted of one BS and a pair of users (one far user and one near user) is studied. Different from the previous researches, we consider the case that between the BS and the far user, there is no direct link, and PS SWIPT technique is applied at the near user to provide energy for forwarding the signal of the far user. The duration of transmission is split into two portions, one for simultaneous wireless energy and information transmission from the BS to the near user, as well as the other one for information forwarding from the near user to the far user. The main contributions of this paper can be summarized as:

1) We consider a multi-carrier cooperative NOMA system where no direct link exists between the far user and the BS. In order to enable the far user to communicate with the BS, the near user plays a role of an energy harvesting relay to forward the signal of the far user.

2) To ensure the QoS requirement of the far user, the number of data bits transmitted to the far user cannot be lower than a given threshold. Subject to the constraints of the energy causality, the minimum data and the transmission power, we aim to maximize the number of data bits received at the near user by jointly optimizing power allocation, subcarrier allocation, time allocation, the PA coefficient and the PS ratio.

3) The optimization problem is non-convex and complex. Before solving the optimization problem, an iterative scheme based on the block-coordinate descent method and the Lagrange

duality method is proposed to check the feasibility of this problem. Then we propose an iterative scheme which adopts the same methods to efficiently obtain a suboptimal solution.

4) Finally, we compare the proposed scheme with three reference schemes which include NOMA schemes with fixed variables and conventional OMA scheme. Simulation results are given to prove the superiority of the proposed new NOMA scheme.

The rest of the paper is organized as follows. In Section 2, the system model and optimization problem formulation are presented. In Section 3, the block-coordinate descent method and the Lagrange duality method are adopted to solve the non-convex and complex optimization problems. Simulation results are given in Section 4, and conclusions follow in Section 5.

2. SYSTEM MODEL AND PROBLEM FORMULATION

We consider a downlink cooperative NOMA system consisting of one BS and a pair of users denoted by U1 (the near user) and U2 (the far user), as shown in **Fig 1.** It is supposed that between the BS and U2, there is no direct link, and U1 acts as a relay for U2 using the energy harvested from the superimposed signal sent from the BS. The total spectrum bandwidth is divided into N subcarriers on average, and the set of these subcarriers is denoted as Ω. Let h_1^i and h_2^i denote the channel coefficients of subcarrier i from BS to U1, and from U1 to U2, respectively. It is assumed that U1 adopts the PS scheme for harvesting energy and decoding information at the same time. The transmission time is normalized to be 1 and split into two phases. In the first phase whose duration is τ, U1 receives the superimposed signal of U1 and U2 coming from the BS and splits it into two portions for harvesting energy and decoding information. Let $\beta \in [0,1]$ denote the PS ratio where a faction of β signal power is split to harvest energy and the remaining 1-β signal power is split to decode information. In the second phase whose duration is 1-τ, U1 forwards the signal of U2 by utilizing the harvested energy. To ensure the QoS requirement of U2, the number of data bits received by U2 cannot be lower than a given threshold denoted as D.

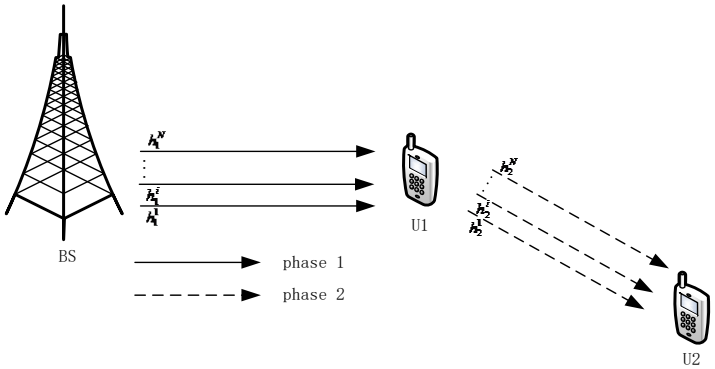

Fig. 1. Downlink cooperative NOMA system model

2.1 Phase 1: Transmission from the BS to U1

On subcarrier i, the BS transmits a superimposed signal denoted as $\sqrt{p_1^i \alpha^i}\, x_1^i + \sqrt{p_1^i (1-\alpha^i)}\, x_2^i$ to U1, where x_1^i is the signal for U1, x_2^i is the signal for U2, α^i is the PA coefficient for x_1^i, and p_1^i is the transmission power of the BS. Assuming that the maximum transmission power

of the BS on all subcarriers is P, thus we have $\sum_{i\in\Omega} p_1^i \le P$. The signal received at U1 is given by

$$y_1^i = h_1^i\left(\sqrt{p_1^i\alpha^i}\,x_1^i + \sqrt{p_1^i\left(1-\alpha^i\right)}x_2^i\right) + n_1^i, \tag{1}$$

where $n_1^i \sim CN\left(0,\sigma_1^2\right)$ denotes the additive white Gaussian noise (AWGN) at U1 on subcarrier i. Using the SWIPT technique, U1 divides y_1^i into two portions which are used to decode information and harvest energy. The harvested energy at U1 can be written as

$$E = \sum_{i\in\Omega}\beta\eta\, p_1^i\left|h_1^i\right|^2\tau, \tag{2}$$

where $\eta\in[0,1]$ denotes the energy conversion efficiency. The signal used for information decoding can be described as

$$y_1^{i(ID)} = \sqrt{1-\beta}\,h_1^i\left(\sqrt{p_1^i\alpha^i}\,x_1^i + \sqrt{p_1^i\left(1-\alpha^i\right)}x_2^i\right) + n_1^i. \tag{3}$$

Assume that the successive interference cancellation (SIC) is applied at U1 to retrieve x_1 and x_2. Specifically, on subcarrier i, U1 first decodes x_2^i and then subtracts it from the superimposed signal to decode x_1^i. Thus, the signal-to-interference-plus-noise ratio (SINR) to decode x_2^i at U1 on subcarrier i can be expressed as

$$\gamma_{1,x_2}^i = \frac{(1-\beta)\left(1-\alpha^i\right)p_1^i\left|h_1^i\right|^2}{(1-\beta)\alpha^i p_1^i\left|h_1^i\right|^2+\sigma_1^2}. \tag{4}$$

The signal-to-noise ratio (SNR) to decode x_1^i at U1 on subcarrier i can be expressed as

$$\gamma_{1,x_1}^i = \frac{(1-\beta)\alpha^i p_1^i\left|h_1^i\right|^2}{\sigma_1^2}. \tag{5}$$

Therefore, the number of data bits decoded for x_1 and x_2 at U1 can be given by

$$D_1 = \tau R_1, \tag{6}$$

and

$$D_{1,x_2} = \tau R_{1,x_2}, \tag{7}$$

respectively, where R_1 and R_{1,x_2} denote the data rate for decoding x_1 and x_2, respectively, at U1, as given by

$$R_1 = \sum_{i\in\Omega}\log_2\left(1+\frac{(1-\beta)\alpha^i p_1^i\left|h_1^i\right|^2}{\sigma_1^2}\right), \tag{8}$$

and

$$R_{1,x_2} = \sum_{i\in\Omega}\log_2\left(1+\frac{(1-\beta)\left(1\text{-}\alpha^i\right)p_1^i\left|h_1^i\right|^2}{(1-\beta)\alpha^i p_1^i\left|h_1^i\right|^2+\sigma_1^2}\right). \tag{9}$$

2.2 Phase 2: Transmission from U1 to U2

U1 utilizes the energy harvested in the first phase to forward x_2 to U2. The signal received at U2 on subcarrier i can be written as

$$y_2^i = \sqrt{p_2^i} h_2^i x_2^i + n_2^i, \tag{10}$$

where $n_2^i \sim CN\left(0, \sigma_2^2\right)$ denotes the AWGN at U2, and p_2^i denotes the transmission power of U1 for forwarding x_2, on subcarrier i. Since the energy consumed by U1 for forwarding x_2 cannot exceed the harvested energy, the energy causality constraint can be given as $\sum_{i\in\Omega} p_2^i (1-\tau) \le \sum_{i\in\Omega} \beta\eta p_1^i \left|h_1^i\right|^2 \tau$. The SNR to decode x_2 at U2 on subcarrier i is given by

$$\gamma_{2,x_2}^i = \frac{p_2^i \left|h_2^i\right|^2}{\sigma_2^2}. \tag{11}$$

Thus, the number of data bits decoded by U2 can be given as

$$D_{2,x_2} = (1-\tau) R_{2,x_2}, \tag{12}$$

where R_{2,x_2} denotes the data rate for decoding x_2 at U2 as given by

$$R_{2,x_2} = \sum_{i\in\Omega} \log_2 \left(1 + \frac{p_2^i \left|h_2^i\right|^2}{\sigma_2^2}\right). \tag{13}$$

Thus, the number of data bits received by U2 can be written as

$$D_2 = \min\left\{D_{1,x_2}, D_{2,x_2}\right\}. \tag{14}$$

To ensure the QoS requirement of U2, the number of data bits received by U2 cannot be lower than the target number of data bits D. Thus, the minimum data constraint requires that $D_2 \ge D$, i.e., $D_{1,x_2} \ge D$ and $D_{2,x_2} \ge D$. The notations are given in **Table 1**.

Table 1. Important Notations

Symbol	Meaning
Ω	Set of subcarriers
h_1^i, h_2^i	Channel coefficients of subcarrier i from BS to U1, and from U1 to U2
p_1^i, p_2^i	Transmission power of the BS and U1
P	Maximum transmission power of the BS on all subcarriers
D	Target number of data bits of U2
τ	Duration of the first phase
β	Proportion of signal power used for energy harvesting
α^i	Proportion of power allocated to the signal of U1 on subcarrier i
η	Energy conversion efficiency
R_1	Data rate of U1
R_{1,x_2}, R_{2,x_2}	Data rate for decoding U2's signal at U1 and U2
D_1	Number of data bits received at U1
D_{1,x_2}, D_{2,x_2}	Number of data bits decoded for U2's signal at U1 and U2
n_1^i, n_2^i	AWGN at U1 and U2 with mean zero and variance σ_1^2 and σ_2^2

2.3 Optimization Problem Formulation

The goal of our paper is to maximize the number of data bits received at U1 by jointly optimizing power allocation, subcarrier allocation, time allocation, the PA coefficient and the PS ratio, subjected to the transmission power constraint, the energy causality constraint and the minimum data constraint. The optimization problem is formulated as

$$(P1): \max_{\beta,\tau,\{\alpha^i\},\{p_1^i\geq 0\},\{p_2^i\geq 0\}} D_1 \tag{15}$$

$$s.t. \sum\nolimits_{i\in\Omega} p_1^i \leq P, \tag{16}$$

$$D_{1,x_2} \geq D, \tag{17}$$

$$D_{2,x_2} \geq D, \tag{18}$$

$$\sum\nolimits_{i\in\Omega} p_2^i (1-\tau) \leq \sum\nolimits_{i\in\Omega} \beta\eta p_1^i \left|h_1^i\right|^2 \tau, \tag{19}$$

$$0 \leq \alpha^i \leq 1, \tag{20}$$

$$0 \leq \beta \leq 1, \tag{21}$$

$$0 \leq \tau \leq 1. \tag{22}$$

The constraint (16) denotes the transmission power constraint of the BS. The constraints (17) and (18) are used to ensure the QoS requirement of U2. The constraint (19) denotes the energy causality constraint which indicates that the energy consumed by U1 for forwarding x_2 cannot exceed the harvested energy. This problem is difficult to solve due to the non-convexity with respect to the optimization variables. In the next sections, we will propose to solve such optimization problem based on the block-coordinate descent method and the Lagrange duality method.

3. RESOURCE ALLOCATION SCHEME

Since the constraints in (17) and (18) may not be satisfied, we first check the feasibility of P1, and then propose a scheme to solve it.

3.1 Problem Feasibility Check

When the number of data bits received by U2 can meet the target number of data bits D, i.e., the constraints in (17) and (18) can be satisfied, P1 is feasible. Thus, the following problem P2 aiming to obtain the maximum number of data bits received by U2 is formulated as

$$(P2): \max_{\beta,\tau,\{\alpha^i\},\{p_1^i\geq 0\},\{p_2^i\geq 0\}} \min\left\{D_{1,x_2}, D_{2,x_2}\right\} \tag{23}$$

$$s.t.\ (16),(19),(20),(21),(22).$$

We can easily verify that the objective function in (23) prefers a smaller α^i. Thus, the optimal α^i for P2 is zero and P2 can be reformulated as

$$(P3): \max_{\beta,\tau,\{p_1^i\geq 0\},\{p_2^i\geq 0\}} \min\left\{D'_{1,x_2}, D_{2,x_2}\right\} \tag{24}$$

$$s.t.\ (16),(19),(21),(22),$$

where $D'_{1,x_2} = \tau R'_{1,x_2}$ and

$$R'_{1,x_2} = \sum\nolimits_{i\in\Omega} \log_2\left(1+\frac{(1-\beta)\,p_1^i\left|h_1^i\right|^2}{\sigma_1^2}\right). \tag{25}$$

P3 is non-convex because of the objective function in (24), and we can solve P3 based on the block-coordinate descent method by iteratively optimizing $\left\{p_1^i\right\}$ and $\left\{p_2^i\right\}$ with given τ and β, and optimizing τ and β with given $\left\{p_1^i\right\}$ and $\left\{p_2^i\right\}$.

Firstly, we optimize $\left\{p_1^i\right\}$ and $\left\{p_2^i\right\}$ with given τ and β. This problem is non-convex, and we first optimize $\left\{p_1^i\right\}$ to obtain the largest D'_{1,x_2} by solving the following problem

$$\max_{\left\{p_1^i\ge 0\right\}} D'_{1,x_2} \tag{26}$$
$$s.t.\ (16).$$

The above problem is convex and can be solved by the Lagrange multiplier method. The solution is

$$p_1^i = \left(\frac{\tau}{\lambda\ln 2} - \frac{\sigma_1^2}{(1-\beta)\left|h_1^i\right|^2}\right)^+, \tag{27}$$

where $(.)^+ = \max\{.,0\}$, λ is the Lagrange multiplier and is numerically obtained from $\sum_{i\in\Omega} p_1^i = P$. Then, we optimize $\left\{p_2^i\right\}$ with given p_1^i in (27) by solving the following problem

$$\max_{\left\{p_2^i\ge 0\right\}} D_{2,x_2} \tag{28}$$
$$s.t.\ (19).$$

The above problem is convex and can be solved similar to the problem in (26). The solution is

$$p_2^i = \left(\frac{1}{\nu\ln 2} - \frac{\sigma_2^2}{\left|h_2^i\right|^2}\right)^+, \tag{29}$$

where ν is the Lagrange multiplier and is numerically obtained from $\sum_{i\in\Omega} p_2^i(1-\tau) = \sum_{i\in\Omega} \beta\eta\, p_1^i\left|h_1^i\right|^2\tau$. After that, we compare D'_{1,x_2} and D_{2,x_2} based on the obtained p_1^i in (27) and p_2^i in (29). If $D'_{1,x_2} \le D_{2,x_2}$, this means the largest D'_{1,x_2} is no larger than D_{2,x_2} and the optimal function value of (26) is equal to the optimal function value of (24), and in this case, the above solution in (27) and (29) is the solution of p_1^i and p_2^i with given τ and β. Otherwise, we obtain the largest D_{2,x_2} in what follows. Let $p_{\min} = \sum_{i\in\Omega} \beta\eta\, p_1^i\left|h_1^i\right|^2\tau$, where p_1^i is obtained in (27). It is easy to verify that a larger $\sum_{i\in\Omega} \beta\eta\, p_1^i\left|h_1^i\right|^2\tau$ leads to a larger D_{2,x_2}. Thus, we allocate all the power to the subcarrier with the maximum channel gain, i.e.,

$$p_1^{i^*} = P,\ p_1^i = 0, i^* = \arg\max_{i\in\Omega}\left|h_1^i\right|^2, i\ne i^*, i\in\Omega. \tag{30}$$

Then, we optimize $\left\{p_2^i\right\}$ to maximize D_{2,x_2} by solving the following problem

$$\max_{\{p_2^i \geq 0\}} D_{2,x_2} \tag{31}$$

$$s.t.\ \sum_{i\in\Omega} p_2^i (1-\tau) \leq \beta\eta P \left|h_1^{i^*}\right|^2 \tau. \tag{32}$$

The above problem is convex and can be solved as

$$p_2^i = \left(\frac{1}{\omega \ln 2} - \frac{\sigma_2^2}{\left|h_2^i\right|^2} \right)^+, \tag{33}$$

where ω is the Lagrange multiplier and is numerically obtained from $\sum_{i\in\Omega} p_2^i (1-\tau) = \beta\eta P \left|h_1^{i^*}\right|^2 \tau$. We then compare D'_{1,x_2} and D_{2,x_2} based on the obtained p_1^i in (30) and p_2^i in (33) again. If $D'_{1,x_2} \geq D_{2,x_2}$, this means the largest D_{2,x_2} is no larger than D'_{1,x_2} and the optimal function value of (31) is equal to the optimal function value of (24), and in this case, the above solution in (30) and (33) is the solution of p_1^i and p_2^i with given τ and β. Otherwise, we obtain the solution of P3 as follows. Let $p_{\max} = \beta\eta P \left|h_1^{i^*}\right|^2 \tau$ and $p = (p_{\min} + p_{\max})/2$, then we optimize $\{p_2^i\}$ by solving the following problem

$$\max_{\{p_2^i \geq 0\}} D_{2,x_2} \tag{34}$$

$$s.t.\ \sum_{i\in\Omega} p_2^i (1-\tau) \leq p. \tag{35}$$

The above problem is convex and can be solved as

$$p_2^i = \left(\frac{1}{\varpi \ln 2} - \frac{\sigma_2^2}{\left|h_2^i\right|^2} \right)^+, \tag{36}$$

where ϖ is the Lagrange multiplier and is numerically obtained from $\sum_{i\in\Omega} p_2^i (1-\tau) = p$. Similarly, we optimize $\{p_1^i\}$ by solving the following problem

$$\max_{\{p_1^i \geq 0\}} D'_{1,x_2} \tag{37}$$

$$s.t.\ \sum_{i\in\Omega} p_1^i = P, \tag{38}$$

$$\sum_{i\in\Omega} \beta\eta p_1^i \left|h_1^i\right|^2 \tau = p. \tag{39}$$

Such problem is convex and can be solved with the Lagrange duality method [39][40]. The Lagrangian of the problem can be written as

$$L\left(\mu_1, \mu_2, \{p_1^i\}\right) = D'_{1,x_2} - \mu_1 \left[\sum_{i\in\Omega} p_1^i - P\right] - \mu_2 \left[\sum_{i\in\Omega} \beta\eta p_1^i \left|h_1^i\right|^2 \tau - p\right], \tag{40}$$

where μ_1 and μ_2 are the non-negative dual variables. The dual function is written as

$$\max_{\{p_1^i \geq 0\}} L\left(\mu_1, \mu_2, \{p_1^i\}\right). \tag{41}$$

Since $L\left(\mu_1, \mu_2, \{p_1^i\}\right)$ is a concave function of p_1^i, the solution of p_1^i can be obtained by setting the first derivative of $L\left(\mu_1, \mu_2, \{p_1^i\}\right)$ with respect to p_1^i to zero as

$$p_1^i = \left(\frac{\tau}{\left(\mu_1 + \mu_2 \beta \eta \tau \left|h_1^i\right|^2\right) \ln 2} - \frac{\sigma_1^2}{(1-\beta)\left|h_1^i\right|^2} \right)^+, \tag{42}$$

where μ_1 and μ_2 can be obtained by the ellipsoid method [41]. Finally, we compare D'_{1,x_2} and D_{2,x_2} based on the obtained p_1^i in (42) and p_2^i in (36). If $D'_{1,x_2} > D_{2,x_2}$, we set $p_{\min} = p$, otherwise we set $p_{\max} = p$. Then, let $p = (p_{\min} + p_{\max})/2$ and obtain p_1^i and p_2^i from (42) and (36) respectively. The above process continues until the gap between the values of D'_{1,x_2} and D_{2,x_2} cannot be further reduced.

Secondly, we optimize τ and β with given $\{p_1^i\}$ and $\{p_2^i\}$. It can be verified that D'_{1,x_2} and D_{2,x_2} are monotonically increasing and decreasing functions of τ, respectively. With any given β, p_1^i and p_2^i, D'_{1,x_2} is smaller than D_{2,x_2} when τ=0 and D'_{1,x_2} is larger than D_{2,x_2} when τ=1. Thus, there exists an optimal point (τ^*, β^*) such that $D'_{1,x_2} = D_{2,x_2}$. From $D'_{1,x_2} = D_{2,x_2}$, we obtain that

$$\tau = \frac{R_{2,x_2}}{R'_{1,x_2} + R_{2,x_2}}. \tag{43}$$

By inserting (43) into the problem in (24), we get

$$\max_{\beta} \frac{R_{2,x_2} R'_{1,x_2}}{R'_{1,x_2} + R_{2,x_2}}. \tag{44}$$

For any $\beta \in [0,1]$, the constraint in (19) requires that

$$\tau \geq \frac{\sum_{i\in\Omega} p_2^i}{\sum_{i\in\Omega} \beta \eta p_1^i \left|h_1^i\right|^2 + \sum_{i\in\Omega} p_2^i}. \tag{45}$$

Therefore, combining (43) with (45), we get the inequality with respect to β denoted as

$$R_{2,x_2} \sum_{i\in\Omega} \beta \eta p_1^i \left|h_1^i\right|^2 \geq \sum_{i\in\Omega} p_2^i R'_{1,x_2}. \tag{46}$$

We can note that the left formula of (46) monotonically increases with β, while the right formula of (46) monotonically decreases with β. Besides, the left formula is smaller than the right formula when β=0 and the left formula is larger than the right formula when β=1. Thus, there is an unique and constant $C \in (0,1)$ such that (46) is satisfied only if $\beta \in [C,1]$. Note that the objective function in (44) is a decreasing function of β. Thus, the optimal β is equal to C, which is obtained by a bisection search within [0, 1] from (46) at equality. Then the value of τ can be obtained from (43).

The iterative procedure of optimizing $\{p_1^i\}$ and $\{p_2^i\}$ with given τ and β and optimizing τ and β with given $\{p_1^i\}$ and $\{p_2^i\}$ terminates until the value of the objective function in P3 cannot be further improved. If the objective function value obtained in P3 reaches the target number of data bits D, P1 is considered to be feasible, otherwise, it is infeasible. **Table 2** outlines the procedure of checking the feasibility of P1.

Table 2. Proposed scheme to check the feasibility of P1.

Initialization: Set τ=0.5 and β=0.5, $\alpha^i = 0$ for $i = 1,...,N$.
repeat
  For fixed τ and β, calculate p_1^i and p_2^i for $i = 1,...,N$ by (27) and (29), respectively.
  if $D'_{1,x_2} > D_{2,x_2}$ **then**
    Let $p_{\min} = \sum_{i\in\Omega} \beta\eta p_1^i \left|h_1^i\right|^2 \tau$ and calculate p_1^i and p_2^i for $i = 1,...,N$ by (30) and (33), respectively.
    if $D'_{1,x_2} < D_{2,x_2}$ **then**
      Let $p_{\max} = \beta\eta P \left|h_1^{i^*}\right|^2 \tau$ and $p = (p_{\min} + p_{\max})/2$.
      repeat
        Calculate p_1^i and p_2^i for $i = 1,...,N$ by (42) and (36), respectively.
        if $D'_{1,x_2} > D_{2,x_2}$ **then**
          Set $p_{\min} = p$.
        else
          Set $p_{\max} = p$.
        end if
        Set $p = (p_{\min} + p_{\max})/2$.
      until the gap between the values of D'_{1,x_2} and D_{2,x_2} cannot be further reduced.
    end if
  end if
  For fixed $\{p_1^i\}$ and $\{p_2^i\}$, let $\beta_{\min}$=0, $\beta_{\max}$=1, and $\beta = (\beta_{\min} + \beta_{\max})/2$.
  repeat
    if $R_{2,x_2} \sum_{i\in\Omega} \beta\eta p_1^i \left|h_1^i\right|^2 \geq \sum_{i\in\Omega} p_2^i R'_{1,x_2}$ **then**
      Set $\beta_{\max} = \beta$.
    else
      Set $\beta_{\min} = \beta$.
    end if
    Set $\beta = (\beta_{\min} + \beta_{\max})/2$.
  until the constraint in (46) is satisfied with a desired accuracy.
  Calculate τ by (43).
  Calculate the number of data bits received by U2 as $\min\{D'_{1,x_2}, D_{2,x_2}\}$.
until the number of data bits received by U2 cannot be further improved.
If the obtained maximum is larger or equal to D, then P1 is feasible. Otherwise, P1 is infeasible.

3.2 Resource allocation scheme

We propose to solve P1 by the block-coordinate descent method and the Lagrange duality method. The solution obtained in **Table 2** is chosen to be a feasible initialization to start the iteration.

We first optimize $\{p_1^i\}$ and $\{p_2^i\}$ with given τ, β and $\{\alpha^i\}$. Such problem is convex and can be solved with the Lagrange duality method. The Lagrangian of the problem can be given as

$$L\left(\lambda_1,\lambda_2,\lambda_3,\lambda_4,\left\{p_1^i\right\},\left\{p_2^i\right\}\right)=D_1-\lambda_1\left[\sum_{i\in\Omega}p_1^i-P\right]-\lambda_2\left[D-D_{1,x_2}\right]-\lambda_3\left[D-D_{2,x_2}\right]-\lambda_4\left[\sum_{i\in\Omega}p_2^i(1-\tau)-\sum_{i\in\Omega}\beta\eta p_1^i\left|h_1^i\right|^2\tau\right], \tag{47}$$

where λ_1, λ_2, λ_3 and λ_4 are the non-negative dual variables. The dual function is written as

$$\max_{\left\{p_1^i\ge 0\right\},\left\{p_2^i\ge 0\right\}} L\left(\lambda_1,\lambda_2,\lambda_3,\lambda_4,\left\{p_1^i\right\},\left\{p_2^i\right\}\right). \tag{48}$$

Since $L\left(\lambda_1,\lambda_2,\lambda_3,\lambda_4,\left\{p_1^i\right\},\left\{p_2^i\right\}\right)$ is a concave function of p_1^i and p_2^i, the solution of p_1^i and p_2^i can be respectively obtained by setting the partial derivative of $L\left(\lambda_1,\lambda_2,\lambda_3,\lambda_4,\left\{p_1^i\right\},\left\{p_2^i\right\}\right)$ with respect to p_1^i or p_2^i to zero as

$$p_1^i=\left(\frac{-b+\sqrt{b^2-4ac}}{2a}\right)^+, \tag{49}$$

$$p_2^i=\left(\frac{\lambda_3}{\lambda_4\ln 2}-\frac{\sigma_2^2}{\left|h_2^i\right|^2}\right)^+, \tag{50}$$

where $\bar{\gamma}=\frac{\sigma_1^2}{(1-\beta)\left|h_1^i\right|^2}$, $a=\alpha^i\left(\lambda_4\beta\eta\left|h_1^i\right|^2-\frac{\lambda_1}{\tau}\right)\ln 2$, $b=\left(\bar{\gamma}+\alpha^i\bar{\gamma}\right)\left(\lambda_4\beta\eta\left|h_1^i\right|^2-\frac{\lambda_1}{\tau}\right)\ln 2+\alpha^i$, $c=\bar{\gamma}^2\left(\lambda_4\beta\eta\left|h_1^i\right|^2-\frac{\lambda_1}{\tau}\right)\ln 2+\lambda_2\bar{\gamma}-\lambda_2\alpha^i\bar{\gamma}+\alpha^i\bar{\gamma}$, and the dual variables λ_1, λ_2, λ_3 and λ_4 can be obtained by the ellipsoid method.

Next, τ is optimized with given $\left\{p_1^i\right\}$, $\left\{p_2^i\right\}$, β and $\left\{\alpha^i\right\}$. From the constraints (17), (18) and (19), the range of τ can be derived as

$$\max\left(\frac{\sum_{i\in\Omega}p_2^i}{\sum_{i\in\Omega}p_2^i+\sum_{i\in\Omega}\beta\eta p_1^i\left|h_1^i\right|^2},\frac{D}{R_{1,x_2}}\right)\le\tau\le 1-\frac{D}{R_{2,x_2}}. \tag{51}$$

Moreover, it is noted that the objective function in (15) is an increasing function of τ. Thus, the optimal τ is obtained as

$$\tau=1-\frac{D}{R_{2,x_2}}. \tag{52}$$

Then, β is optimized with given $\left\{p_1^i\right\}$, $\left\{p_2^i\right\}$, τ and $\left\{\alpha^i\right\}$. From (19), we can draw that

$$\beta\ge\frac{\sum_{i\in\Omega}p_2^i(1-\tau)}{\sum_{i\in\Omega}\eta p_1^i\left|h_1^i\right|^2\tau}. \tag{53}$$

Since the objective in (15) is a decreasing function of β, the optimal β is obtained as

$$\beta=\frac{\sum_{i\in\Omega}p_2^i(1-\tau)}{\sum_{i\in\Omega}\eta p_1^i\left|h_1^i\right|^2\tau}. \tag{54}$$

At last, we optimize $\{\alpha^i\}$ with given τ, β, $\{p_1^i\}$ and $\{p_2^i\}$. The constraint (17) can be rewritten as $\sum_{i\in\Omega}\tau\log_2\left((1-\beta)\alpha^i p_1^i|h_1^i|^2+\sigma_1^2\right)\le\sum_{i\in\Omega}\tau\log_2\left((1-\beta)p_1^i|h_1^i|^2+\sigma_1^2\right)$-$D$ and the objective function in (15) can be rewritten as $\sum_{i\in\Omega}\tau\log_2\left((1-\beta)\alpha^i p_1^i|h_1^i|^2+\sigma_1^2\right)$-$N\tau\log_2\sigma_1^2$. Let

$$t^i=\tau\log_2\left((1-\beta)\alpha^i p_1^i|h_1^i|^2+\sigma_1^2\right). \tag{55}$$

Therefore, P1 is reformulated as

$$\max_{\{t^i\}}\sum_{i\in\Omega}t^i\text{-}N\tau\log_2\sigma_1^2 \tag{56}$$

$$s.t.\ \sum_{i\in\Omega}t^i\le\sum_{i\in\Omega}\tau\log_2\left((1-\beta)p_1^i|h_1^i|^2+\sigma_1^2\right)\text{-}D, \tag{57}$$

$$N\tau\log_2\sigma_1^2\le\sum_{i\in\Omega}t^i\le\sum_{i\in\Omega}\tau\log_2\left((1-\beta)p_1^i|h_1^i|^2+\sigma_1^2\right). \tag{58}$$

It is easy to verify that $\sum_{i\in\Omega}\tau\log_2\left((1-\beta)p_1^i|h_1^i|^2+\sigma_1^2\right)$-$D\ge N\tau\log_2\sigma_1^2$. Thus, we obtain the maximum value of the objective function in (56) as long as (57) is taken into equal. Let $t^i=\tau\log_2\left((1-\beta)p_1^i|h_1^i|^2+\sigma_1^2\right)$-$\frac{D}{N}$. Then, the optimal α^i can be expressed as

$$\alpha^i=\frac{2^{\frac{t^i}{\tau}}-\sigma_1^2}{(1-\beta)p_1^i|h_1^i|^2}. \tag{59}$$

The iterative procedure of optimizing $\{p_1^i\}$ and $\{p_2^i\}$ with given τ, β and $\{\alpha^i\}$, optimizing τ with given $\{p_1^i\}$, $\{p_2^i\}$, β and $\{\alpha^i\}$, optimizing β with given $\{p_1^i\}$, $\{p_2^i\}$, τ and $\{\alpha^i\}$, optimizing $\{\alpha^i\}$ with given $\{p_1^i\}$, $\{p_2^i\}$, τ and β terminates until the number of data bits received at U1 cannot be further improved. In summary, the proposed resource allocation scheme is outlined in **Table 3**.

Table 3. Proposed resource allocation scheme for cooperative SWIPT NOMA.

1: Set the initial values of τ, β, $\{p_1^i\}$, $\{p_2^i\}$ and $\{\alpha^i\}$ using the results in **Table 2**.
2: **repeat**
3: Initialize λ_1, λ_2, λ_3 and λ_4.
4: **repeat**
5: For fixed τ, β, and $\{\alpha^i\}$, calculate p_1^i and p_2^i for $i=1,...,N$ by (49) and (50), respectively.
6: Update λ_1, λ_2, λ_3 and λ_4 by the ellipsoid method.
7: **until** λ_1, λ_2, λ_3 and λ_4 converge to a prescribed accuracy.
8: For fixed β, $\{p_1^i\}$, $\{p_2^i\}$ and $\{\alpha^i\}$, calculate τ by (52).
9: For fixed τ, $\{p_1^i\}$, $\{p_2^i\}$ and $\{\alpha^i\}$, calculate β by (54).
10: For fixed τ, β, $\{p_1^i\}$ and $\{p_2^i\}$, calculate α^i for $i=1,...,N$ by (59).
11: Calculate the number of data bits received by U1 as D_1.
12: **until** the number of data bits received by U1 cannot be further improved.

4. SIMULATION RESULTS

This section presents some simulation results to prove the performance of the proposed NOMA scheme. In the simulation, both the distance between the BS and U1, U1 and U2 are assumed to be 3m and we set the energy conversion efficiency $\eta = 0.5$. The total system bandwidth is 10MHz and it is equally divided into 10 subcarriers. Without loss of generality, the large-scale path loss is modeled by $10^{-3} d^{-2.5}$, where d denotes the distance. Moreover, we assume that the channels of all subcarriers follow the standard Rayleigh fading and the noise power at U1 and U2 is set to -90dBm, i.e., $\sigma_1^2 = \sigma_2^2 = -90dBm$.

For comparison, we provide three reference schemes. In the first reference scheme named as NOMA with fixed β, the PS ratio is set to 0.5 and other variables are optimized similar to the proposed NOMA scheme. In the second scheme named as NOMA with fixed α, the PA coefficient is set to 0.2 while the other variables are also optimized similar to the proposed NOMA scheme. In the third reference scheme named as conventional OMA scheme, the TDMA mode is adopted to serve U1 and U2 with variable optimization method similar to the proposed NOMA scheme.

Fig. 2 presents the number of U1 data bits versus the maximum transmission power of the BS P for different schemes, where the target number of U2 data bits D is set to 10Mb. On the one hand, we can observe from the **Fig. 2** that the number of U1 data bits grows with the increase of P and as P increases, the growth rate of U1 data slows down. This is reasonable, because a larger P enables U1 to harvest more energy and results in a higher number of transmitted data bits for U1. Besides, the U1 data in (6) is a logarithmic function of P which leads to the slower growth at the higher P. On the other hand, it is also shown that the proposed NOMA scheme outperforms the other schemes. This proves the superiority of the proposed NOMA scheme. This is because the proposed NOMA scheme harvests the energy of two users' signals together, while conventional OMA scheme can only collect the energy of one user.

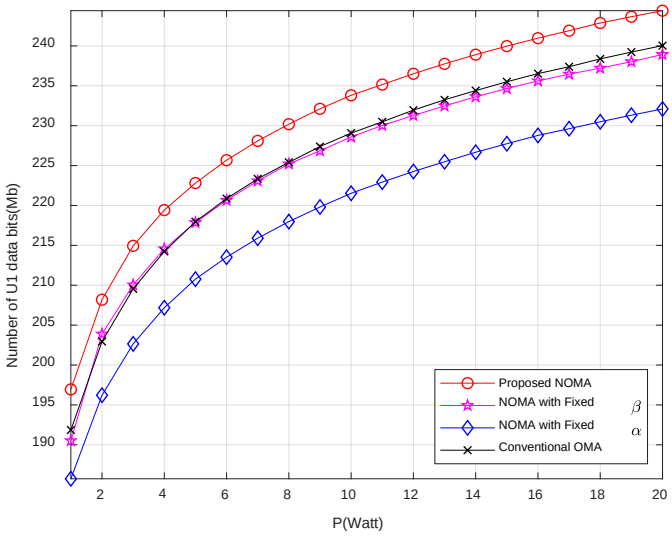

Fig. 2. Number of U1 data bits versus P.

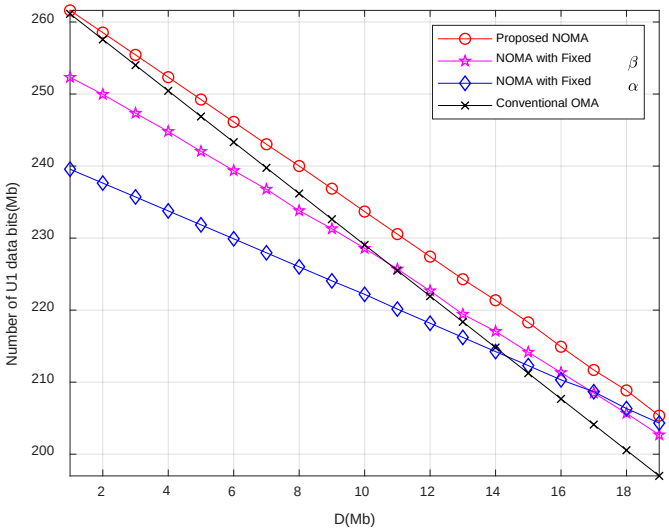

Fig. 3. Number of U1 data bits versus D.

Fig. 3 shows the number of U1 data bits versus the target number of U2 data bits D for different schemes, where the maximum transmission power of the BS P is set to 10W. It can be observed that the number of U1 data bits decreases as the target number of U2 data bits D increases. This is because a higher D makes U2 take more resources which reduces the resources allocated to U1. We can observe that the numbers of U1 data bits of NOMA with fixed α or β schemes are much lower than the proposed NOMA scheme when D is small, while the performance of conventional OMA scheme is similar to the proposed NOMA scheme. This is because allocating a large amount of power to U2's signal and splitting too much power for forwarding U2's signal are both unreasonable when D is small. As D increases, the performance gap between NOMA with fixed α or β schemes and the proposed scheme reduces, while the performance gap between conventional OMA scheme and the proposed scheme gets larger. The reasons are two-fold. Firstly, when D gets larger, U1 is required to harvest more energy for forwarding the signal of U2. The NOMA schemes provide the higher gain in the case of a higher D because of the simultaneous energy harvesting of two users, compared to the conventional OMA scheme. Secondly, it is reasonable to split a large amount of power for forwarding U2's signal when D is large. It is worth mentioning that although the performances of NOMA with fixed α scheme approaches the proposed NOMA scheme when D is high, NOMA with fixed α has no feasible solution in the very high D regime.

In **Fig. 4**, we present the optimal values of α and β obtained by the proposed scheme versus the maximum transmission power of the BS P, where the target number of U2 data bits D is set to 10Mb. From **Fig. 4** (a) we can observe that the optimal value of α increases with the increase of P. This is because a larger P makes it easier to satisfy the transmission requirement of U2, and U1 can get a greater proportion of power to improve its performance. **Fig. 4** (b) shows that the optimal value of β decreases as P increases. The reason is that as P increases, a larger proportion of signal power received by U1 can be split for information decoding to improve the performance of U1.

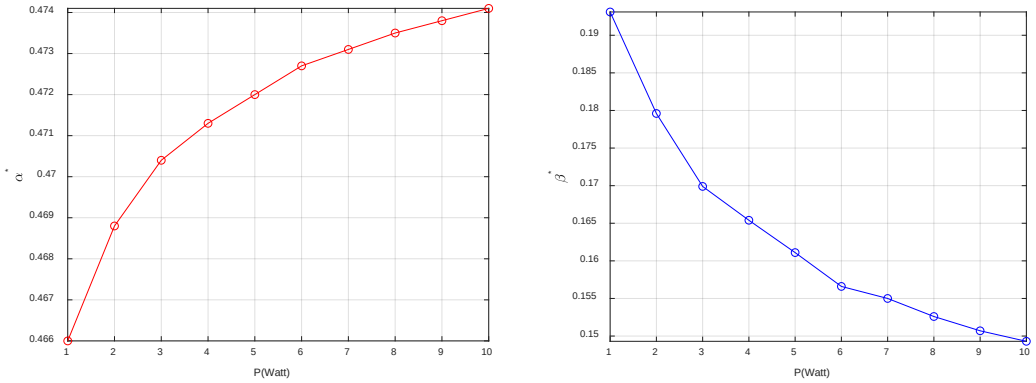

(a) Optimal α (b) Optimal β

Fig. 4. Optimal α and β obtained by the proposed scheme versus P.

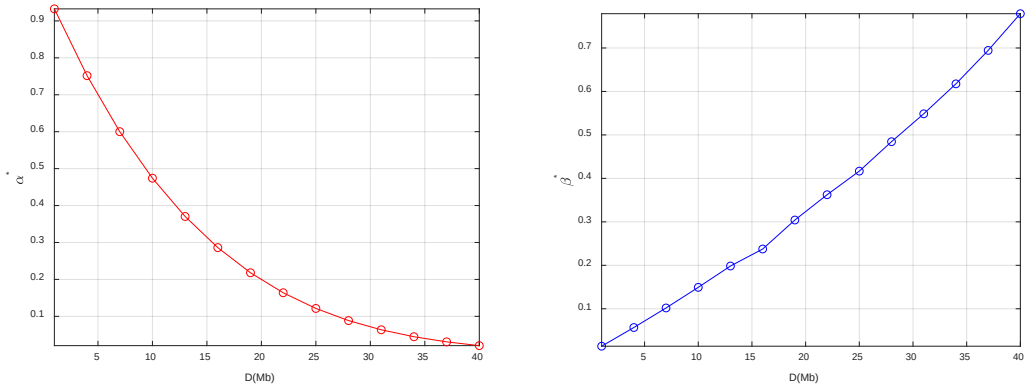

(a) Optimal α (b) Optimal β

Fig. 5. Optimal α and β obtained by the proposed scheme versus D.

In **Fig. 5**, we depict the optimal values of α and β obtained by the proposed scheme versus the target number of U2 data bits D, where the maximum transmission power of the BS P is set to 10W. We can find that as D increase, the optimal value of α decreases, while the optimal value of β increases. This is reasonable, because when D gets larger, the power allocated to the signal of U2 and the energy harvested by U1 need to increase to meet U2's transmission target. Besides, it is noted that for $D<19$, the optimal values of α and β gradually approach the value of $\alpha=0.2$ and $\beta=0.5$ fixed in reference NOMA schemes. This can reasonably explain why the performance of NOMA with fixed α or β schemes approaches the performance of the proposed scheme with the increase of D, as shown in **Fig. 3**.

5. Conclusions

In summary, we considered a downlink multi-carrier cooperative NOMA system, which consists of one BS and a pair of the near and far users. It was assumed that between the BS and the far user, there is no direct link, and SWIPT is applied at the near user to harvest energy for forwarding the signal of the far user. Considering constraints of the energy causality, the minimum data and the transmission power, we maximized the number of data bits transmitted

to the near user by jointly optimizing power allocation, subcarrier allocation, time allocation, the PA coefficient and the PS ratio. First of all, an iterative scheme based on the block-coordinate descent method and the Lagrange duality method was proposed to check the feasibility of the optimization problem. After that, another iterative scheme based on the same methods was proposed to achieve a suboptimal solution of the problem. Finally, simulation results demonstrated that our proposed scheme outperforms the reference NOMA schemes with fixed PS ratio or PA coefficient and the conventional OMA scheme.

References

[1] Haijun Zhang, Fang Fang, Julian Cheng, Keping Long, Wei Wang and Victor C. M. Leung, "Energy-Efficient Resource Allocation in NOMA Heterogeneous Networks," *IEEE Wireless Communications*, vol. 25, no. 2, pp. 48-53, April, 2018. Article (CrossRef Link).

[2] Yuanwei Liu, Zhijin Qin, Maged Elkashlan, Zhiguo Ding, Arumugam Nallanathan and Lajos Hanzo, "Nonorthogonal Multiple Access for 5G and Beyond," *Proceedings of the IEEE*, vol. 105, no. 12, pp. 2347-2381, December, 2017. Article (CrossRef Link).

[3] Haijun Zhang, Ning Yang, Keping Long, Miao Pan, George K. Karagiannidis and Victor C. M. Leung, "Secure Communications in NOMA System: Subcarrier Assignment and Power Allocation," *IEEE Journal on Selected Areas in Communications*, vol. 36, no. 7, pp. 1441-1452, July, 2018. Article (CrossRef Link).

[4] Zhiguo Ding, Yuanwei Liu, Jinho Choi, Qi Sun, Maged Elkashlan, Chih-Lin I and H. Vincent Poor, "Application of Non-Orthogonal Multiple Access in LTE and 5G Networks," *IEEE Communications Magazine*, vol. 55, no. 2, pp. 185-191, February, 2017. Article (CrossRef Link).

[5] Haijun Zhang, Yu Qiu, Keping Long, George K. Karagiannidis, Xianbin Wang and Arumugam Nallanathan, "Resource Allocation in NOMA-Based Fog Radio Access Networks," *IEEE Wireless Communications*, vol. 25, no. 3, pp. 110-115, June, 2018. Article (CrossRef Link).

[6] Zhiguo Ding, Xianfu Lei, George K. Karagiannidis, Robert Schober, Jinhong Yuan and Vijay K. Bhargava, "A Survey on Non-Orthogonal Multiple Access for 5G Networks: Research Challenges and Future Trends," *IEEE Journal on Selected Areas in Communications*, vol. 35, no. 10, pp. 2181-2195, October, 2017. Article (CrossRef Link).

[7] Haijun Zhang, Baobao Wang, Chunxiao Jiang, Keping Long, Arumugam Nallanathan, Victor C. M. Leung and H. Vincent Poor, "Energy Efficient Dynamic Resource Optimization in NOMA Systems," *IEEE Transactions on Wireless Communications*, vol. 17, no. 9, pp. 5671-5683, September, 2018. Article (CrossRef Link).

[8] Qi Sun, Shuangfeng Han, Chin-Lin I and Zhengang Pan, "On the Ergodic Capacity of MIMO NOMA Systems," *IEEE Wireless Communications Letters*, vol. 4, no. 4, pp. 405-408, August, 2015. Article (CrossRef Link).

[9] Zhiguo Ding, Fumiyuki Adachi and H. Vincent Poor, "The Application of MIMO to Non-Orthogonal Multiple Access," *IEEE Transactions on Wireless Communications*, vol. 15, no. 1, pp. 537-552, January, 2016. Article (CrossRef Link).

[10] Qi Sun, Shuangfeng Han, Zhikun Xu, Sen Wang, Chih-Lin I and Zhengang Pan, "Sum Rate Optimization for MIMO Non-Orthogonal Multiple Access Systems," in *Proc. of IEEE Wireless Communications and Networking Conference*, pp. 747-752, June, 2015. Article (CrossRef Link).

[11] Zhiguo Ding, Pingzhi Fan and H. Vincent Poor, "Impact of User Pairing on 5G Nonorthogonal Multiple-Access Downlink Transmissions," *IEEE Transactions on Vehicular Technology*, vol. 65, no. 8, pp. 6010-6023, August, 2016. Article (CrossRef Link).

[12] Yi Zhang, Qian Yang, Tong-Xing Zheng, Hui-Ming Wang, Ying Ju and Yue Meng, "Energy Efficiency Optimization in Cognitive Radio Inspired Non-Orthogonal Multiple Access," in *Proc. of IEEE 27th Annual International Symposium on Personal, Indoor, and Mobile Radio Communications*, pp. 1-6, December, 2016. Article (CrossRef Link).

[13] Sultangali Arzykulov, Galymzhan Nauryzbayev, Theodoros A. Tsiftsis and Mohamed Abdallah, "Outage Performance of Underlay CR-NOMA Networks," in *Proc. of 10th International Conference on Wireless Communications and Signal Processing*, pp. 1-6, December, 2018. Article (CrossRef Link).
[14] Zhiguo Ding, Mugen Peng and H. Vincent Poor, "Cooperative Non-Orthogonal Multiple Access in 5G Systems," *IEEE Communications Letters*, vol. 19, no. 8, pp. 1462-1465, August, 2015. Article (CrossRef Link).
[15] Jung-Bin Kim and In-Ho Lee, "Capacity Analysis of Cooperative Relaying Systems Using Non-Orthogonal Multiple Access," *IEEE Communications Letters*, vol. 19, no. 11, pp. 1949-1952, November, 2015. Article (CrossRef Link).
[16] Zhiguo Ding, Huaiyu Dai and H. Vincent Poor, "Relay Selection for Cooperative NOMA," *IEEE Wireless Communications Letters*, vol. 5, no. 4, pp. 416-419, August, 2016. Article (CrossRef Link).
[17] Jooncherl Ho and Minho Jo, "Offloading Wireless Energy Harvesting for IoT Devices on Unlicensed Bands," *IEEE Internet of Things Journal*, vol. 6, no. 2, pp. 3663-3675, April, 2019. Article (CrossRef Link).
[18] Suzhi Bi, Chin Keong Ho and Rui Zhang, "Wireless Powered Communication: Opportunities and Challenges," *IEEE Communications Magazine*, vol. 53, no. 4, pp. 117-125, April, 2015. Article (CrossRef Link).
[19] Ding Xu and Qun Li, "Cooperative Resource Allocation in Cognitive Radio Networks with Wireless Powered Primary Users," *IEEE Wireless Communications Letters*, vol. 6, no.5, pp. 658-661, October, 2017. Article (CrossRef Link).
[20] Hongyuan Gao, Waleed Ejaz and Minho Jo, "Cooperative Wireless Energy Harvesting and Spectrum Sharing in 5G Networks," *IEEE Access*, vol. 4, pp. 3647-3658, July, 2016. Article (CrossRef Link).
[21] Ding Xu and Qun Li, "Resource Allocation for Secure Communications in Cooperative Cognitive Wireless Powered Communication Networks," *IEEE Systems Journal*, pp. 1-12, 2018. Article (CrossRef Link).
[22] Jun Huang, Cong-Cong Xing, Yi Qian and Zygmunt J. Haas, "Resource Allocation for Multicell Device-to-Device Communications Underlaying 5G Networks: A Game-Theoretic Mechanism with Incomplete Information," *IEEE Transactions on Vehicular Technology*, vol. 67, no. 3, pp. 2557-2570, March, 2018. Article (CrossRef Link).
[23] Dong-Woo Lim, Joonhyuk Kang, Chang-Jae Chun and Hyung-Myung Kim, "Joint Transmit Power and Time-Switching Control for Device-to-Device Communications in SWIPT Cellular Networks," *IEEE Communications Letters*, vol. 23, no. 2, pp. 322-325, February, 2019. Article (CrossRef Link).
[24] Jun Huang, Shuai Huang, Cong-Cong Xing, and Yi Qian, "Game-Theoretic Power Control Mechanisms for Device-to-Device Communications Underlaying Cellular System," *IEEE Transactions on Vehicular Technology*, vol. 67, no. 6, pp. 4890-4900, Jan, 2018. Article (CrossRef Link).
[25] Lav R. Varshney, "Transporting Information and Energy Simultaneously," in *Proc. of IEEE International Symposium on Information Theory, Toronto, Canada*, pp. 1612-1616, July, 2008. Article (CrossRef Link).
[26] Jun Huang, Cong-Cong Xing and Chonggang Wang, "Simultaneous Wireless Information and Power Transfer: Technologies, Applications, and Research Challenges," *IEEE Communications Magazine*, vol. 55, no. 11, pp. 26-32, Nov, 2017. Article (CrossRef Link).
[27] Jing Zhang, Qingjie Zhou, Derrick Wing Kwan Ng and Minho Jo, "Optimal Energy Efficiency Fairness of Nodes in Wireless Powered Communication Networks," *Sensors*, vol. 17, no. 9, pp. 2125, September, 2017. Article (CrossRef Link).
[28] Ding Xu and Qun Li, "Resource Allocation in Cognitive Wireless Powered Communication Networks with Wirelessly Powered Secondary Users and Primary Users," *Science China Information Sciences*, vol. 62, no. 2, pp. 29303, 2018. Article (CrossRef Link).

[29] Ali A. Nasir, Xiangyun Zhou, Salman Durrani and Rodney A. Kennedy, "Relaying Protocols for Wireless Energy Harvesting and Information Processing," *IEEE Transactions on Wireless Communications*, vol. 12, no. 7, pp. 3622-3636, July, 2013. Article (CrossRef Link).
[30] Rui Zhang and Chin Keong Ho, "MIMO Broadcasting for Simultaneous Wireless Information and Power Transfer," *IEEE Transactions on Wireless Communications*, vol. 12, no. 5, pp. 1989-2001, May, 2013. Article (CrossRef Link).
[31] Xun Zhou, Rui Zhang and Chin Keong Ho, "Wireless Information and Power Transfer in Multiuser OFDM Systems," *IEEE Transactions on Wireless Communications*, vol. 13, no. 4, pp. 2282-2294, April, 2014. Article (CrossRef Link).
[32] Ding Xu and Hongbo Zhu, "Outage Minimized Resource Allocation for Multiuser OFDM Systems with SWIPT," *IEEE Access*, vol. 7, pp. 79714-79725, June, 2019. Article (CrossRef Link).
[33] Mateen Ashraf, Ju-Wook Jang, Jong-Ki Han and Kyung Geun Lee, "Capacity Maximizing Adaptive Power Splitting Protocol for Cooperative Energy Harvesting Communication Systems," *IEEE Communications Letters*, vol. 22, no. 5, pp. 902-905, May, 2018. Article (CrossRef Link).
[34] Lu Liu, Zhifei Zhang, Chao Shen, Jie Gong and Tsung-Hui Chang, "Wireless Powered Cooperative Non-Orthogonal Multiple Access Transmission," in *Proc. of IEEE International Conference on Communications Workshops*, pp. 1-6, July, 2018. Article (CrossRef Link).
[35] Yinghui Ye, Yongzhao Li, Dan Wang and Guangyue Lu, "Power Splitting Protocol Design for the Cooperative NOMA with SWIPT," in *Proc. of IEEE International Conference on Communications*, pp. 1-5, July, 2017. Article (CrossRef Link).
[36] Yanqing Xu, Chao Shen, Zhiguo Ding, Xiaofang Sun, Shi Yan, Gang Zhu and Zhangdui Zhong, "Joint Beamforming and Power-Splitting Control in Downlink Cooperative SWIPT NOMA Systems," *IEEE Transactions on Signal Processing*, vol. 65, no. 18, pp. 4874-4886, September, 2017. Article (CrossRef Link).
[37] Yuanwei Liu, Zhiguo Ding, Maged Elkashlan and H. Vincent Poor, "Cooperative Non-Orthogonal Multiple Access in 5G Systems with SWIPT," in *Proc. of 23rd European Signal Processing Conference*, pp. 1999-2003, December, 2015. Article (CrossRef Link).
[38] Lin Zhang, Jiaqi Liu, Ming Xiao, Gang Wu, Ying-Chang Liang and Shaoqian Li, "Performance Analysis and Optimization in Downlink NOMA Systems With Cooperative Full-Duplex Relaying," *IEEE Journal on Selected Areas in Communications*, vol. 35, no. 10, pp. 2398-2412, October, 2017. Article (CrossRef Link).
[39] Stephen Boyd and Lieven Vandenberghe, *Convex Optimization*, Cambridge University Press, 2004. Article (CrossRef Link).
[40] Ding Xu and Qun Li, "Joint Power Control and Time Allocation for Wireless Powered Underlay Cognitive Radio Networks," *IEEE Wireless Communications Letters*, vol. 6, no. 3, pp. 294-297, June, 2017. Article (CrossRef Link).
[41] Robert G. Bland, Donald Goldfarb and Michael J. Todd, "Feature Article—The Ellipsoid Method: A Survey," *Operations Research*, vol. 29, no. 6, pp. 1039–1091, December, 1981. Article (CrossRef Link).

Longqi Wang received the B.E. degree in Communication Engineering from the Nanjing University of Posts and Telecommunications, Nanjing, China, in 2017. She is currently pursuing master's degree at the school of Communication and Information Engineering in the Nanjing University of Posts and Telecommunications. Her current research interests include non-orthogonal multiple access, cooperative communications and energy harvesting.

Ding Xu received the Ph.D. degrees from the Beijing University of Posts and Telecommunications, Beijing, in 2013. He is currently an Associate Professor at the Nanjing University of Posts and Telecommunications, Nanjing, China. He has published more than 90 technical papers in scientific journals and at international conferences. His research interests include cognitive radio, wireless-powered communications, physical-layer security, mobile edge computing, and non-orthogonal multiple access. He serves as an Associate Editor for IEEE ACCESS. He is a senior member of IEEE.